CFD ANALYSES OF FLUID FLOW AND HEAT TRANSFER IN PATTERNED ROLL-BONDED ALUMINIUM PLATE RADIATORS

A. WITRY[1] and M. H. Al-HAJERI [2] and Ali A. BONDOK[3]

[1] Senior Automotive CFD Analyst, Automotive R & D Centre**,** Windsor, Ontario, Canada

[2] Mechanical Power Engineering, Faculty of Technical Studies, Kuwait, hajeri@paaet.edu.kw

[3] Research Scientist, AB Research and Development, Windsor, Ontario, Canada

ABSTRACT

The thermal performance of an automotive radiator plays an important role in the performance of an automobile's cooling system and all other associated systems. For a number of years, this component has suffered from little attention with very little changing in its manufacturing cost, operation and geometry. As opposed to the old tubular heat exchanger configurations used in automotive radiators, plate heat exchangers currently form the backbone of today's process industry with their advanced performance reaching levels tubular heat exchangers can only dream of.

The Aluminum roll-bonding technique widely used in manufacturing the cooling compartments for domestic refrigeration units is one of the cheapest methods for heat exchanger manufacturing. Using this technique, it is possible to manufacture a wide range of heat exchanger configurations that can help augment heat transfer whilst reducing pressure drops. CFD results obtained for a patterned plate heat exchanger using the CFD code FLUENT show tremendous levels of possible performance improvement on both sides the heat exchanger.

For the internal flow, heat transfer augmentation caused by the repetitive impingement against the dimple obstructions renders such geometries equal to those of aerospace industry pin-fins whilst lowering pressure drops due to the wider cross-sectional areas. For the external flows, the wider and wavy nature of the surface area increases heat transfer leaving the addition of extra surface roughness add-ons optional.

INTRODUCTION

For over 60 years now, little change has occurred to the design and manufacturing of automotive radiators. However, better, cheaper and yet far more advanced designs of heat exchangers are available to this industry today mainly developed for the process industries. Using Computational Fluid Dynamics (CFD), it is hereby sought to model the flow and heat transfer performance characteristics for one such design as a possible replacement for the conventional automotive radiator.

Using suitable Aluminium sheets, a technique used to manufacture evaporators for domestic refrigerators called Aluminium Roll-Bonding Technique (ARBT) is used to pressure-fuse two suitably thin Aluminium sheets against each other. With the help of an anti-adhesive profile on the inner side of the two sheets, it is possible to form a pattern of internal flow passages to the required shape by applying relatively high internal air pressures blowing the sheets out to form a variety of internal flow passages shapes. The high air pressures create internal flow-passages that match the adhesive applied areas, whilst also creating a similar pattern on the plate's external surfaces.

The ease of such a technique and the near-absence of any welding spots along with mass-productivity capabilities for such methods led in the past to the application of such methods to use in domestic fridges. The resulting heat exchanger panels can be made into any shape, can withstand medium-pressures and represent a great manufacturing cost saving. A discussion of a particular design approach discussed below shows a wide range of possibilities for enhancing the thermal performance whilst lowering pressure drop tolls. Witry (1996) shows the possibility of using such plates for a variety of other purposes including those related to power generation facilities.
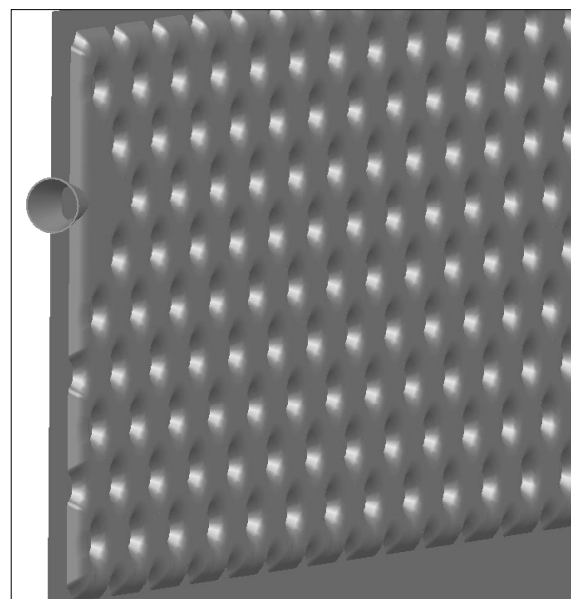
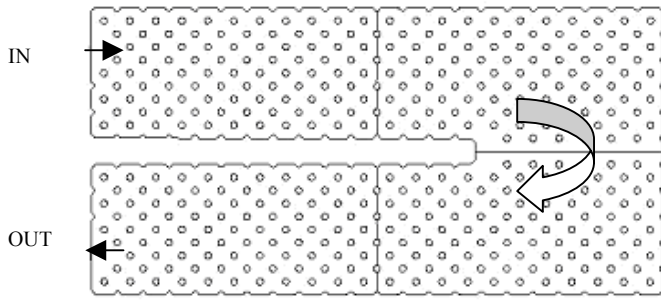

Figure 1: Partial Dimple Plate Geometry

Figure 2: Overall Tube Side Flow Arrangement

Figure 1 shows one such design where successive rows and columns of equally spaced staggered dimples help provide high levels of heat transfer augmentation on both sides of the heat exchanger and a wide cross sectional area that would lower pressure drops. The internal flows' wall angle is 45°. A 180° turn in flow direction also allows the flow to have a longer thermal length whilst adding extra "effective" heat transfer areas, figure 2.

The wider cross-sectional area on both sides of the plate allows the flow(s) lower velocities giving lower pressure drops for the critical internal flow side than that for its tubular counterpart heat exchanger geometry. At the inlet, outlet and 180° bend, a number of dimples have been removed to allow the flow a chance to re-distribute itself without causing high pressure losses and to serve as an internal collector-distributor, figure 3. Further modifications to this geometry could include adding pin-like fins on the outer plate surface to add roughness and to help completely destroy any re-circulations and boundary layer flows generated there.
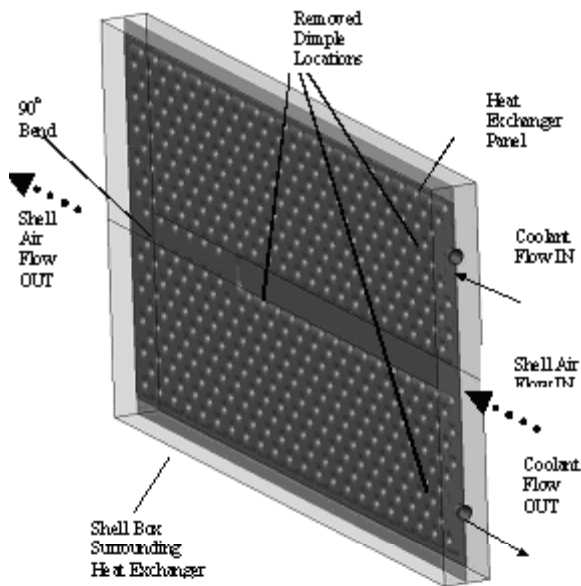

Figure 3: The Simulated Setup

Witry (1999) shows that whilst a similar plate heat exchanger design produced a higher pressure drop than that for a long serpentine passage heat exchanger plate with 5 of two branch split bends, pressure drop increases also increased conservatively whilst increasing heat transfer by folds. From a heat transfer point of view, the

plate's waviness produces a roughness-like effect on the outside surfaces whilst not affecting heat transfer due to the wide cross sectional area for that flow passage. Witry et al (1998) further showed that such plates can be used for a variety of purposes and can withstand acceptable levels of fouling. An added advantage to this technique is Aluminium's capability to withstand corrosion.

A number of such plates can be assembled in parallel at a wide range of spacings to provide increasing load handling capabilities. Alternatively, the plates can be cut and shaped to any particular dimensions necessary whilst being careful regarding allowable working pressures. With the help of CFD, it is possible to estimate the essential parameters in the study of heat exchangers namely, the pressure drops and heat transfer coefficients.

Holman (1992) gives the heat transfer coefficient on either side of the heat exchanger by;

$$E = h . A . (T_F - T_W) \tag{1}$$

Therefore;

$$h = \frac{E}{A.(T_F - T_W)} \tag{2}$$

Ignoring the thermal resistance of any thin conducting metal sheet between the two fluid sides, the same reference gives the overall heat transfer coefficient as;

$$E = U. A_o . LMTD \tag{3}$$

Where U is the overall heat transfer heat coefficient, LMTD is the Log-Mean-Temperature-Difference, see reference for definition). Based on A_o, the U value may be calculated from CFD results using;

$$U_O = \frac{1}{\dfrac{A_o}{A_i} \dfrac{1}{h_i} + \dfrac{1}{h_o}} \tag{4}$$

where A_o / A_i is the area ratio of 1.23385 giving the amount of extra heat transfer due to the area increases caused by surface waviness. This way, CFD results with hi and ho results can be directly used to calculate the overall heat transfer coefficient. The joint counter/parallel flow setup used in this particular geometry helps increase the available thermal length of the internal flow streams, adding extra temperature change to that side. Therefore, the LMTD values obtained from counter and parallel flow arrangements are seriously different, therefore, it is their averaged value that will be used throughout this work's results reporting process.

BACKGROUND

The estimation of a heat exchanger's thermal performance at the early design stage can be achieved using two approaches, analytical and computational. Using analytical models, the internal flow through the successive rows of dimples can be modelled as pin-fins or tube banks whilst external flows can be simulated as the flow of a fluid over a wavy surface or perforated roughened surface. Witry

(1999) used such approaches to model a number of plate heat exchanger geometries using the test data provided. Whilst such methods proved their robustness for calculating heat transfer, the same can not be said about pressure drops.

Witry (1999) also used CFD techniques and the k- ε turbulence model to simulate the problems using overall 2D and smaller regional 3D models per heat exchanger side for two external side flow spacings of 30 and 40mm. Heat transfer and pressure drop results obtained there correlated very well with those data obtained from experiment, therefore, raising hopes to the capacity for solving such problems in a singular 3D mesh representing the whole domain using today's better computational resources.

CFD MODEL SETUP, PROCEDURES AND BOUNDARY CONDITIONS

Two, coarse and dense, separate CFD meshes were created for each side of the heat exchanger to establish grid dependency effects. Figures 4 and 5 show boundary meshes for the shell and tube sides respectively. Wherever possible, extensive use of symmetry boundary condition planes around the models to concentrate available computational power to modeling an increased number of small mesh elements at key features. Therefore, only a quarter of the three dimensional shell tube domains are modeleld using FLUENT's segregated, implicit, 3D steady state solver with incompressible heat transfer. Table 1 shows a listing of boundary conditions and setup criteria employed per geometry.

The mesh is created using a CATIA 4 CAD file in the ICEM-CFD tetra module. Once the resulting mesh successfully passes all ICEM-CFD's mesh quality checks, the mesh is exported to FLUENT where the boundary condition and physical data are setup. The main considerations here are factors like mesh skewness and the y+ values for better fluid flow and heat transfer predictions respectively. Once a converged solution is obtained, the initial mesh is adapted for better predictions of velocity, pressure and temperature gradients causing a rapid increase in elements count. The resulting "refined" mesh is solved again for inspection of grid dependency and better result's qualities.

The separate fluid flow, pressure drop and heat transfer data shell and tube results are processes in an Excel spreadsheet using standard theory. Equation 4 is used to "merge" ho and hi results for both sides of the heat exchanger using the area ratio given to obtain the overall heat transfer coefficients (U). The pumping power consumed, especially for the coolant fluid, is predicted using the product of pressure drops and volumetric flow rates.

Category	Parameter	Internal (Tube)	External (Shell)
Turbulence Modelling	Turbulence Model	k-ε	k- ε
	Wall Function	NEWF	NEWF
Main Geometrical Features	As Used By The CAD Model	45° angled walls with symmetry through the plate's centre plane	30mm distance between plate surface and opposite walls
Physical Properties	Fluid @ 20^oC	Water	Air
	Density [kg/m^3]	998.2	1.225
	Viscosity [kg/m.s]	0.001003	0.0242
	Thermal Conductivity [W/m.^{o}C]	0.6	0.0242
	Cp [J/kg.^{o}C]	4182	1006.3
Tetra Mesh	Coarse (No. of Cells)	869778	3098977
	Dense (No. of Cells)	2097739	4481498
	Dense Mesh Max. Angular Skewness	0.848	0.771
	Dense Mesh HT Area (m^2)	0.7344 (total real)	0.90605
	No. of Symmetry Planes	1	2
	Y^+ (at 1kg/s Flowrate): Averaged	30.523	23.98
Boundary Conditions	Wall (^{o}C) Temperatures	20	120
	Inlet (^{o}C) Temperatures (= $T_{Reference}$)	120	20
	Inlet (%) Turbulence Intensity	3.5	3
	Inlet (m) Hydraulic Diameter	0.0254	0.03

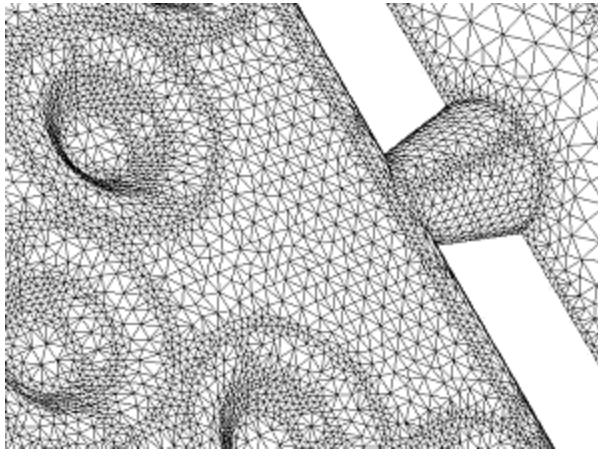**Table 1:** Setup and Boundary Conditions Table

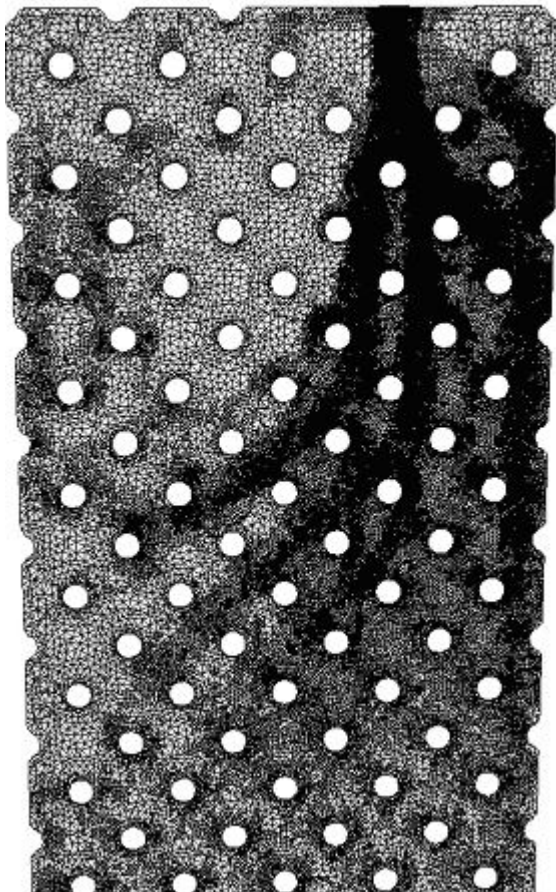**Figure 5:** Shell Side Surface Mesh (Near Inlet Plane)

Figure 6: Tube Side Surface Mesh (Near Inlet)

Figures 5 and 6 show the modified (dense) meshed geometries for the shell and tube sides, respectively. On the tube side, successive mesh adaptations at high velocity, heat transfer, Y+ and pressure drop gradient regions gave the high concentrations of cells, seen in figure 6, around the flow paths originally obtained by solving a coarse

mesh, giving a 241% larger mesh size. This increase in mesh size only produced a maximum 0.57% enhancement in pressure drop and heat transfer predictions quality, therefore, deeming the solution as grid independent.

Similarly, figure 5 shows a 214% increase in shell side mesh size obtained using smaller size cells near the heat transferring walls and at the sharp edges around the geometry only produced a 1.78% enhancement in heat transfer and pressure drop predictions deeming the solution again as grid independent. All results will use the adapted versions of the mesh.
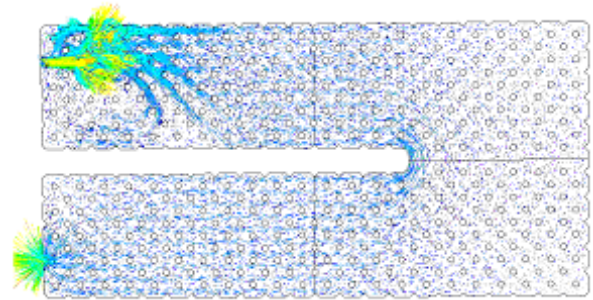

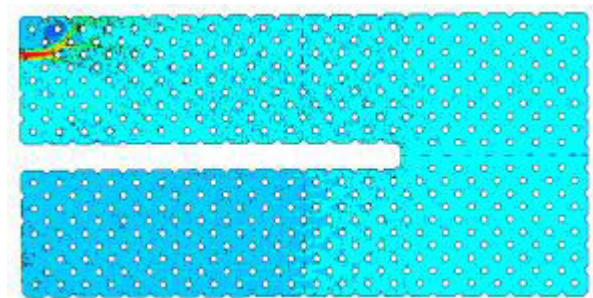**Figure 7:** Internal Flow Velocity Vectors

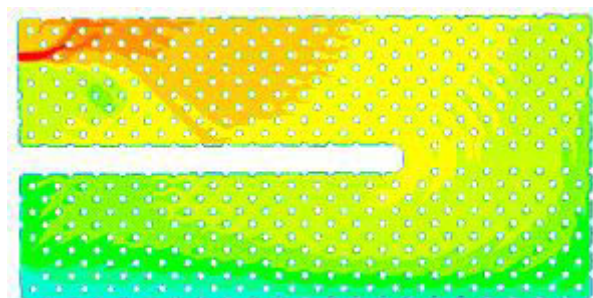**Figure 8:** Internal Flow Pressure Distributions

Figure 9: Internal Flow Temperature Distributions

RESULTS AND DISCUSSION

To increase the benefit from this work, CFD results obtained here will be compared to their testing equivalent using suppliers performance data for a 1998 luxury range automotive radiator with a 27mm coolant side diameter.

Figure 7 shows the velocity vectors field for water flow inside the dimple plate. High inlet flow impingement pressure losses are still evident here and in figure 8 where the high inlet pressure is lost due to the direct hit against the dimple facing the inlet and to the sudden enlargement in cross-sectional area. This indicates the need for more dimples to be removed for a longer hydraulic length from the flow's path. Beyond the inlet region, the flow begins to form major re-circulatory flows whilst trying to find the shortest way towards the outlet. This leads to the generation of a low-pressure region near the inlet jet causing high flow shear levels.

Closer inspection of flow profiles around the dimples show the 3-dimensionality of the problem. Whilst most of the flow going around the dimple will have to re-direct itself, another considerable amount of flow near dimples is dependent on large wavy surface areas in the vicinity. It is hereby expected that these flows perform the bulk of the heat transferring energy exchanging due to the large heat conducting areas, repetitive boundary layer eliminations and turbulence levels involved.

Figure 7 further shows the bulk of coolant's flow to move in a uni-directional manner. This usually tempts workers to create analytical models and solve problems in a 1-D fashion. This, however, is not advised here since it is clearly evident that such regions only form a small part of the overall picture. Further inconsistencies are found around the 90° bend where the repetitive columns of dimples upstream the bend and the removal of a complete row of dimples failed to provide for a uniform flow around the bend. Nevertheless, figure 8 shows a pressure wave of uniform shape and depth forming near the downstream leg's mid-section possibly indicating some form of flow uniformity.

The high coolant velocities lead to exceedingly high heat transfer coefficients especially near the inlet. Here, a rapid temperature drop takes place in the vicinity of areas where the flow came to lower velocities next to high velocity regions. High convection levels reduce the temperature of re-circulating streams rapidly showing a number of similarities to the pressure loss characteristics with no flow mixing taking place at the 90° bend opposite to initial predictions.

Figure 10 shows the external air flow velocity vectors at reduced speeds as the airflows over the dimpled valleys. No reverse flow re-circulation can be noticed here leading to speculation of the existence of high (core) and low flow speed domains. This reduces the amount of heat pickup from the external surface by the cold air and will lead to lower convection values.
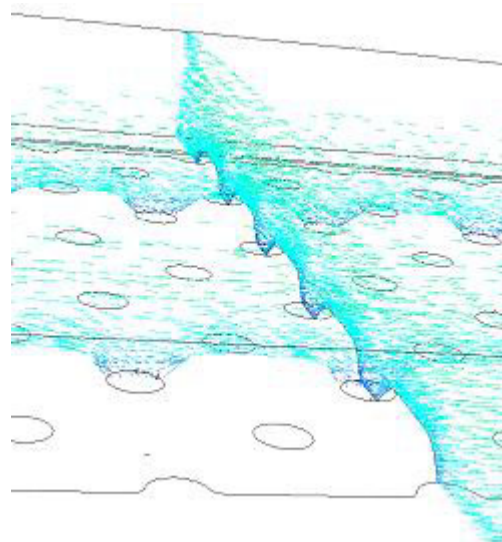

Figure 10: Shell Side Air Flow Velocity Vectors Across Two Perpendicular Cross-Sections Halfway Downstream the Flow
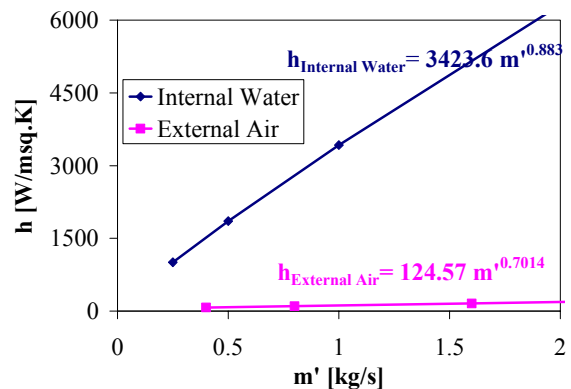

Figure 11: Averaged Heat Transfer Coefficients per Heat Exchanger Flow Side

These observations are confirmed in figure 11 above. The extreme levels of flow impingement, vortex shedding and surface rubbing observed inside the plate out-weigh the external air shell side flow. Partially, this can be also attributed to the use of Water, a better heat transfer agent inside the plate. Since the external surface represents a smooth wavy channel, further measures can be introduced to encourage mixing on the shell side that would allow h values there further allowing U values to increase.
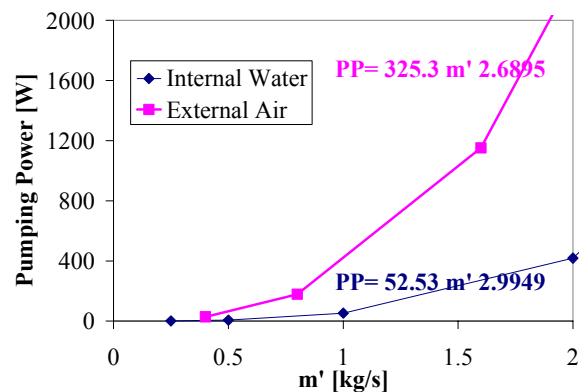

Figure 12: Dimple Plate Heat Exchanger Pumping Power

257

Figure 12 show the need for higher pumping power on the air side than that necessary on the coolant (liquid) side. This is density related and is caused by the large quantities of volumetric air side flow rates in comparison to those observed on the coolant side.

The joint heat transfer performance of individual h values on either side of the heat exchanger are evident in figure 13. Here, it can be clearly seen that increases in air side heat transfer coefficients are critical to any relevant increase in U values. It is therefore recommended to introduce a form of shell side mixing turbulators to increase mixing, possibly in the form of cross bars. This is expected to occur naturally without intervention in an automotive underhood due to the effects of flow non-uniformities caused by neighboring components indicating the possibility of higher overall heat transfer coefficients upon use of such radiators.
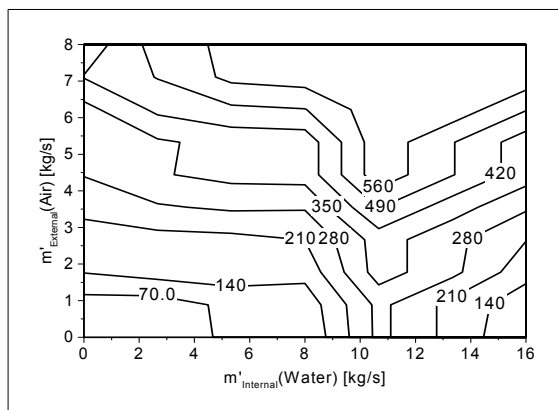

Figure 13: Overall Heat Transfer Coefficients in [W/m^2.K]

Nevertheless, the U values shown in figure 13 are still higher than the expected values for their finned tube counter parts with water/steam inside and air outside the heat exchanger arrangement, Holman (1992). The increase in dimple plate heat transfer surface areas further indicates the possibility to gain increased heat transfer levels.
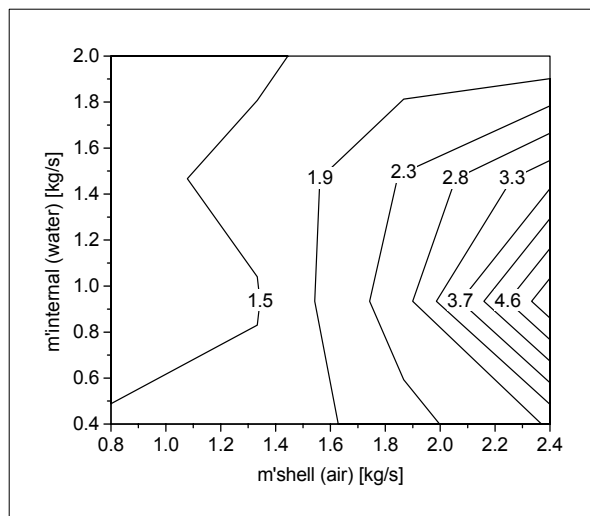

Figure 14: Heat Transfer Enhancement above That For A 1998 Luxury Car Radiator

The increase in heat transfer performance is shown in figure 14 when compared to test data results for a 1998 luxury car radiator. With the already high levels of h values observed on the water side, increases in shell side air flow rates tend to be the main factor controlling performance improvement here. This is especially true when considering that the common radiator today makes extensive use of fins to promote heat transfer on the shell side, a measure that is absent here.

CONCLUSIONS

The dimple plate heat exchanger design presented here is merely a single design with many common performance enhancement measures remaining unused. Whilst the addition of some form of air side turbulators should prove immensely useful, the current design of the heat exchanger promises the following:

- Higher heat transfer levels
- Lower pressure drop levels
- Lower overall vehicle drag
- Smaller size radiators
- Cheaper to manufacture

The heat transfer levels indicated shown here are expected to rise in a real vehicle. The authors had used similar heat exchangers at the same working pressures. Nevertheless, special attention should be given to reducing the permissible operating internal pressure due to safety considerations. Attention should also be given to coolant flow velocities inside the plate due to flow impingement and erosion/corrosion considerations.

REFERENCES

AL-WITRY A 'Thermal Performance of Roll-Bonded Aluminium Plate Heat Exchanger Panels For Use In Ocean Thermal Energy Conversion', Ph.D. Thesis, The University of Nottingham, U.K., 1999.

AL-WITRY A., AROUSSI A. et al 'Heat Exchangers For Low Grade Waste Heat', pp159-163, Solar Engineering Conference, ASME, San Antonio, 1996.

HOLMAN J. P. 'Heat Transfer' , 7th Edition SI units, McGraw-Hill Publishing, 1992.